GA-A24869

INTEGRATED PLASMA CONTROL FOR HIGH PERFORMANCE TOKAMAKS

by
D.A. HUMPHREYS, R.D. DERANIAN, J.R. FERRON,
R.J. JAYAKUMAR, R.D. JOHNSON,
R.R. KHAYRUTDINOV, R.J. LAHAYE, J.A. LEUER,
M.A. MAKOWSKI, B.G. PENAFLOR,
M.L. WALKER, and A.S. WELANDER

OCTOBER 2004

DISCLAIMER

GA-A24869

INTEGRATED PLASMA CONTROL FOR HIGH PERFORMANCE TOKAMAKS

by
D.A. HUMPHREYS, R.D. DERANIAN, J.R. FERRON,
R.J. JAYAKUMAR,[‡] R.D. JOHNSON,
R.R. KHAYRUTDINOV,[£] R.J. LAHAYE, J.A. LEUER,
M.A. MAKOWSKI,[‡] B.G. PENAFLOR,
M.L. WALKER, and A.S. WELANDER

[‡]Lawrence Livermore National Laboratory, Livermore, California
[£]TRINITI Laboratory, Troitsk, Russia

This is a preprint of a paper to be presented at the 20th IAEA Fusion Energy Conference, Vilamoura, Portugal, November 1–6, 2004 and to be printed in the Proceedings.

Work supported by
U.S. Department of Energy
under Contract No. DE-FC02-04ER54698

GENERAL ATOMICS PROJECT 30200
OCTOBER 2004

INTEGRATED PLASMA CONTROL FOR HIGH PERFORMANCE TOKAMAKS

D.A. Humphreys,[1] R.D. Deranian,[1] J.R. Ferron,[1] R.J. Jayakumar,[2] R.D. Johnson,[1] R.R. Khayrutdinov,[3] R.J. LaHaye,[1] J.A. Leuer,[1] M.A. Makowski,[2] B.G. Penaflor,[1] M.L. Walker,[1] and A.S. Welander,[1]

[1]General Atomics, San Diego, California
[2]Lawrence Livermore National Laboratory, Livermore, California, USA
[3]TRINITI Laboratory, Troitsk, Russia

Abstract. Sustaining high performance in a tokamak requires controlling many equilibrium shape and profile characteristics simultaneously with high accuracy and reliability, while suppressing a variety of MHD instabilities. Integrated plasma control, the process of designing high-performance tokamak controllers based on validated system response models and confirming their performance in detailed simulations, provides a systematic method for achieving and ensuring good control performance. For present-day devices, this approach can greatly reduce the need for machine time traditionally dedicated to control optimization, and can allow determination of high-reliability controllers prior to ever producing the target equilibrium experimentally. A full set of tools needed for this approach has recently been completed and applied to present-day devices including DIII-D, NSTX and MAST. This approach has proven essential in the design of several next-generation devices including KSTAR, EAST, JT-60SC, and ITER. We describe the method, results of design and simulation tool development, and recent research producing novel approaches to equilibrium and MHD control in DIII-D.

1. Introduction

Plasma control in high performance devices such as DIII-D must simultaneously regulate highly shaped plasma equilibria with large vertical stability growth rates and many operating regime characteristics such as thermal stored energy or plasma beta, plasma density, and both the configuration and effectiveness of the divertor. In order to operate at high normalized beta, various MHD instabilities must also be controlled, often in concert with operating regime and equilibrium control. For example, one algorithm used in DIII-D for neoclassical tearing mode (NTM) suppression adjusts the plasma equilibrium to align the electron cyclotron current drive (ECCD) deposition location with the NTM island location [1]. In order to enable operation in high performance regimes, DIII-D has developed and demonstrated such coordinated control as well as a suite of enabling tools for designing and testing control algorithms. We refer to the design approach used to systematically develop and test these control algorithms as integrated plasma control. Section 2 describes the integrated plasma control approach and the suite of enabling tools which have been developed at DIII-D to implement the method. In addition to DIII-D, this approach is being successfully applied to control development at various devices which are using or will use the DIII-D plasma control system (PCS) [2], including NSTX [3], KSTAR [4], and EAST [5].

Accurate models of the axisymmetric plasma response to conductor currents in particular are important for design of equilibrium shape, position, and stability controllers. The DIII-D shape control scheme, based on regulation of flux at selected points at the plasma boundary [6], has driven development of an extremely accurate plasma response model which accounts for nonrigid displacements of fluid elements and resistive flux penetration, including the plasma boundary. Previous response models based on rigid vertical and radial plasma displacements have shown unacceptable inaccuracies in predicting the flux response of several boundary control points [7]. Section 3 describes the derivation and application of this model, based on a linear perturbation of the Grad-Shafranov equation.

The need for tokamaks to extract maximum performance from the power supplies and PF-coil set often leads to operation near or at power supply current and voltage limits. For example, the DIII-D tokamak operates in proximity to one or more current limits in some part of virtually

every discharge. Such discharges typically avoid early termination by virtue of extensive offline operator tuning. However, linear, multivariable, model-based shape controllers designed predictively to avoid the need for tuning will, in general, attempt to extend coil current demands to reduce errors to zero, even when currents are near limits. Section 4 presents the generic tokamak problem of current-limiting and discusses some nonlinear solutions being implemented on DIII-D.

An essential requirement of achieving sustained operation at high values of normalized beta in a tokamak is NTM stabilization. In DIII-D, the NTM has been stabilized by applying localized ECCD on the resonant surface at which islands form [1]. This has been accomplished by regulating the island/ECCD alignment through variation of the plasma position or the toroidal field, using the island amplitude inferred from magnetic measurements as a feedback parameter reflecting the degree of alignment. Recently the realtime equilibrium reconstruction algorithm (RTEFIT [8]) used for shape control has been upgraded to provide realtime safety factor (q) calculation based on motional Stark effect (MSE) and magnetic measurements. Section 5 describes the NTM suppression system at DIII-D, including recent upgrades that make use of this new realtime q-profile reconstruction capability in the DIII-D PCS to maintain alignment after the mode has been suppressed, or to prevent the mode onset altogether. Concluding remarks are made in Section 6, along with comments on application of integrated plasma control to ITER [9].

2. Integrated Plasma Control

Figure 1 shows elements of the integrated plasma control approach used at DIII-D. The actual multi-cpu hardware/software system, which ordinarily provides plasma control for DIII-D in experimental operations (conceptually connecting 1A to 2A through switch S1), can also be connected to a detailed simulation of the device (1A to 2B through S1 and S2) in order to test and confirm operation of specific algorithm implementations prior to use in an experiment. When the PCS hardware is occupied while being used for experimental operation, its software alone ("PCS Simulator," 1B to 2B through S2) can be run on a separate platform against the same tokamak simulation in a mode which models the timing and dynamics of the actual hardware and network. This latter closed loop simulation is essential for next generation device designs for which either a hardware version of the PCS or the actual tokamak is lacking. Simulations used for controller or PCS testing can include a nonlinear core plasma model consisting of an adaptation of the DINA [10] 1 1/2-D resistive axisymmetric MHD and transport code. These simulations include models of all key elements of the control system, a subset of which (particularly the linear ones) are used in multivariable control design. In order to provide the necessary degree of controller reliability, it is essential that these models be validated against experiments across a broad range of operating regimes.

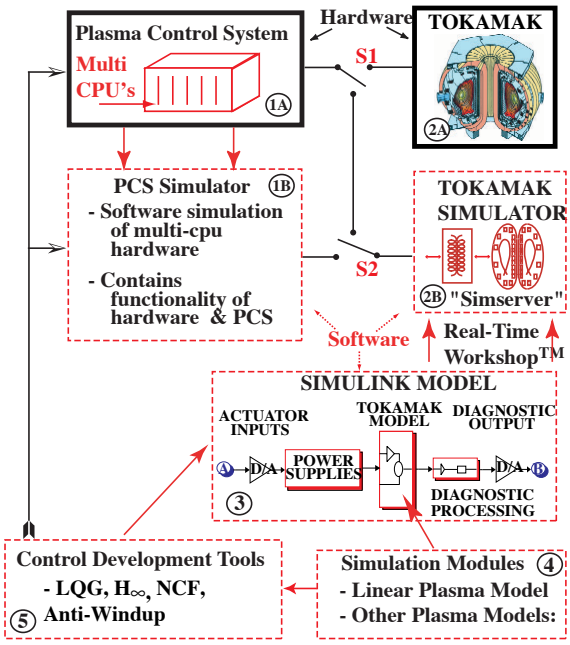

Fig. 1. Elements of the integrated plasma control approach developed for DIII-D. Key elements include the highly flexible digital PCS, detailed system simulations which can be coupled to the PCS, and validated models for all main subsystems impacting DIII-D control.

These elements, now in operational use at DIII-D, comprise a unique and complete integrated plasma control tool set for design and commissioning of high reliability controllers.

3. Nonrigid, Resistive Plasma Response Modeling

The integrated plasma control approach has also allowed development of novel high accuracy axisymmetric control algorithms for DIII-D in regimes where plasma boundary response and nonlinear constraints must be considered. Study of dynamic shape response has shown that the resistive response of edge currents plays a significant role in boundary control in DIII-D. Demand for high accuracy shape controllers on DIII-D has thus led to development of new plasma models for control design that accurately represent the linear nonrigid resistive plasma response. While other linear nonrigid response models have proven successful in describing realistic plasma deformation, the present derivation is specifically designed for integration with resistive plasma response, and explicitly includes the response to thermal variation through a simple but experimentally verified kinetic closure.

A nonrigid linear plasma response can be easily included in the standard formalism for the axisymmetric MHD tokamak system response, described by Faraday's Law circuit equations for all conductors in the system [11–13]:

$$M_{ss}\dot{I}_s + R_{ss}I_s + M_{sp}\dot{I}_p + \frac{\partial\psi_s}{\partial\xi_R}\dot{\xi}_R + \frac{\partial\psi_s}{\partial\xi_Z}\dot{\xi}_Z = V_s \quad , \tag{1}$$

and a resistive plasma can be included in the circuit description via

$$M_{pp}\dot{I}_p + R_{pp}I_p + M_{ps}\dot{I}_s + \frac{\partial\psi_p}{\partial\xi_R}\dot{\xi}_R + \frac{\partial\psi_p}{\partial\xi_Z}\dot{\xi}_Z = 0\,, \tag{2}$$

where I_s is the vector of perturbed conductor currents, I_p is the vector of perturbed plasma fluid element currents, V_s is the vector of perturbed conductor voltages, ψ_s is the vector of perturbed flux at conductors, ξ_R and ξ_Z are plasma fluid element major radial and vertical displacement vectors respectively, R denotes a resistance matrix, M denotes a mutual inductance matrix, and subscripts "p" and "s" denote plasma and stabilizing conductors respectively. Under the quasi-equilibrium massless-plasma assumption, the linearized radial (F_R) and vertical (F_Z) force balance at each fluid element are given respectively by:

$$\delta F_R = 0 = \frac{\partial F_R}{\partial I_s}I_s + \frac{\partial F_R}{\partial I_p}I_p + \frac{\partial F_R}{\partial \xi_R}\xi_R + \frac{\partial F_R}{\partial \xi_z}\xi_z + \frac{\partial F_R}{\partial W_{th}}W_{th}\ \delta F_R^{app} + \delta F_R^{hoop} \quad , \tag{3}$$

$$\delta F_Z = 0 = \frac{\partial F_Z}{\partial I_s}I_s + \frac{\partial F_Z}{\partial I_p}I_p + \frac{\partial F_Z}{\partial \xi_R}\xi_R + \frac{\partial F_Z}{\partial \xi_z}\xi_z + \frac{\partial F_Z}{\partial W_{th}}W_{th}\ \delta F_z^{app} \quad , \tag{4}$$

where F_R^{app} and F_z^{app} are forces due to applied fields, F_R^{hoop} is the radial hoop force, and W_{th} is the perturbed thermal stored energy (scalar or vector representing local energy density values). Eqs. (1) through (4) yield a system of equations describing the dynamic evolution of toroidal conductors and plasma fluid element currents, I_p. The plasma circuit equation Eq. (2) (which allows each fluid element current to vary according to the local neoclassical resistivity) accounts for resistive magnetic flux diffusion through the plasma. This requires that the plasma response be calculated for conserved current at each fluid element.

The elements of the force balance equation are calculated by linearly perturbing the Grad-Shafranov equation

$$\Delta^*\psi = -\mu_0 R^2 p' - FF' = -\mu_0 R j_\varphi \tag{5}$$

while conserving fluid (grid) element thermal energy. We assume a perturbation of the original equilibrium by a change in the applied field ($\delta\psi^{app}$) that also leads to changes in the stream functions. The difference between the perturbed and original equilibrium is:

$$\Delta^*(\psi_1 - \psi_0) = -\mu_0 R^2\left(p_1'(\psi_1) - p_0'(\psi_0)\right) - \left(F_1F_1'(\psi_1) - F_0F_0'(\psi_0)\right) \tag{6}$$

Radial and vertical force balance are explicitly assured through the constraints

$$\delta F_R^{app} = \delta\left(\iint_{plasma} 2\pi R dR dZ j_\varphi B_Z^{app}\right) = -\delta F_{hoop}, \quad \text{and} \quad \delta F_Z^{app} = \delta\left(\iint_{plasma} 2\pi R dR dZ j_\varphi B_R^{app}\right) = 0, \quad (7)$$

which provide the terms in Eqs. (3) and (4). In order to couple Eq. (1) to the resistive plasma current evolution equation, Eq. (2), the total plasma current must be conserved in the plasma response,

$$\delta I_p = \iint_{plasma} \delta j_\varphi dR dZ + \oint_{boundary} j_{edge}\left(\delta\psi - \delta\psi_{xpt}\right)/|\nabla\psi| ds = 0. \quad (8)$$

while the plasma displacement responses to plasma current variation [second pair of in Eqs. (3) and (4)] are calculated separately.

The total kinetic energy is similarly conserved in the plasma response

$$\delta W_{th} = \iint_{plasma} \delta p 3\pi R dR dZ = 0, \quad (9)$$

while the responses to explicit variation in thermal energy [last terms in Eqs. (3) and (4)] are calculated separately. This constraint is chosen as an approximation to the more complex transport-dependent situation, recognizing that the timescales of interest are not short enough for full adiabatic energy conservation, but are not long enough that thermal energy loss is significant. Moreover, using the thermal stored energy as an input to the system allows the actual measured stored energy or auxiliary heating effects to be taken into account directly.

While the nominal plasma response to externally applied flux assumes explicit plasma current and kinetic energy conservation, these quantities do in fact vary and affect the plasma response. Accordingly, we allow plasma currents in fluid elements to evolve in accordance with their resistive response, Eq. (2). The plasma thermal stored energy is an exogenous variable which in practice is modified by ohmic and auxiliary power input, as well as by transport variations. An exogenous variable is an independent input to the dynamic equations, whose evolution is therefore not described by those equations but must be specified (e.g. from measurements). The effect of stored energy variation is calculated through the same perturbed equilibrium formalism, but enters as the exogenous parameter shown in Eqs. (3) and (4), and affects the dynamic evolution Eqs. (1) and (2) through the resulting plasma displacement responses, ξ_R and ξ_Z.

The accuracy of this approach in reproducing DIII-D plasma responses can be seen in Figs. 2 and 3. Figure 2 shows a significantly nonrigid radial shape variation experiment performed in DIII-D, compared with the model prediction. The plasma boundary predicted by the model response closely matches the experimental equilibrium reconstruction. Corresponding flux measurements and model predictions at four points around the vacuum vessel also show excellent dynamic agreement. Figure 3 shows a similar comparison of model and experimental response for a large, nonrigid vertical displacement. The degree of nonrigidity can be seen in the difference between the vertical displacement of the X-point compared with the plasma top. Again the agreement between experiment and model prediction is excellent.

4. Nonlinear Control Algorithms

While the new models of Section 3 have increased linear controller accuracy, study of fundamental control in tokamaks has revealed important limitations to linear control when operating near coil limits. Fig. 4 shows the envelope of maximum and minimum currents allowed in each PF coil for a typical DIII-D equilibrium, which must be exceeded in several coils in order to exactly satisfy the corresponding shape request (even though the differences between the exact shape request and an operationally acceptable shape may be extremely small). These limits arise from either power supply or magnetic force constraints. A linear controller will seek to produce zero error, and will thus tend to exceed the current limits. Solutions for

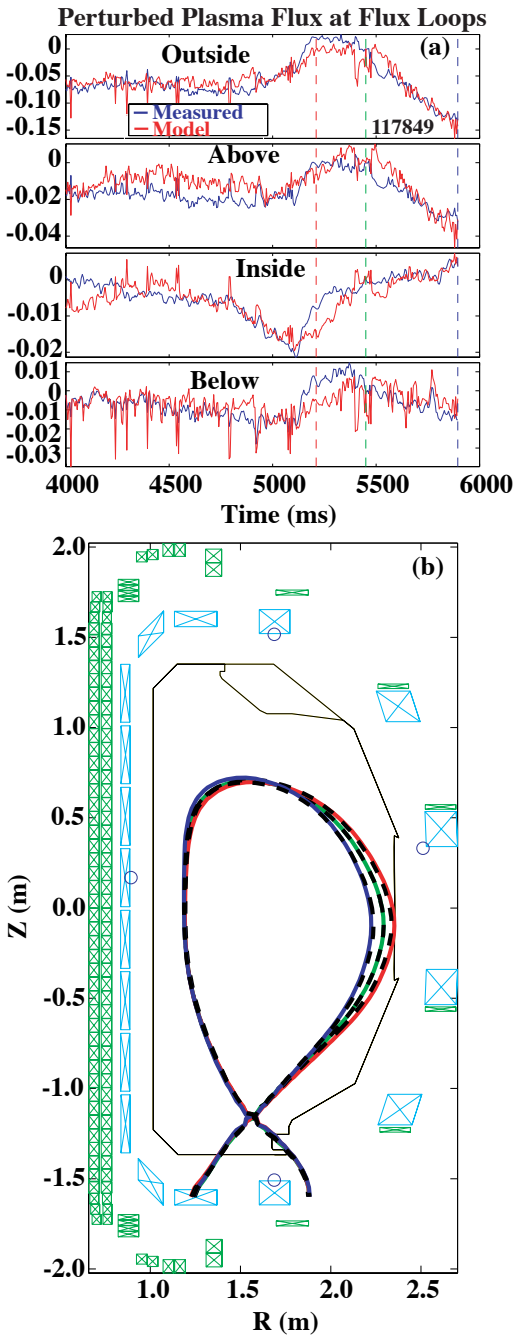

Fig. 2. Linear nonrigid model accurately predicts nonrigid radial displacement of plasma (outboard) boundary produced in DIII-D experiment.

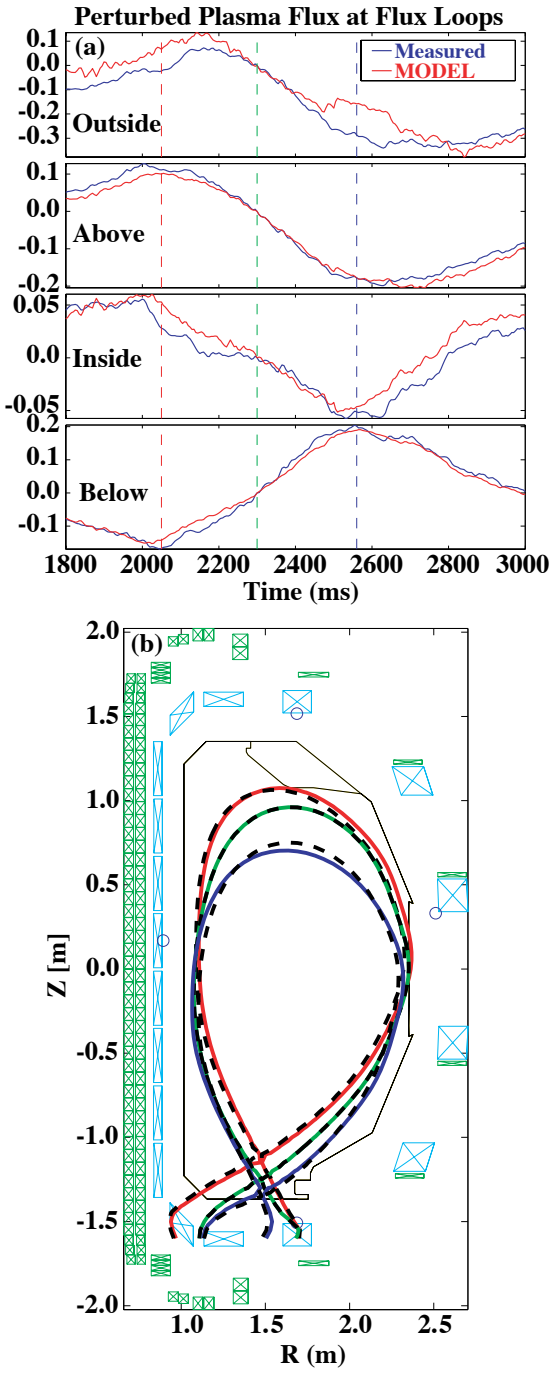

Fig. 3. Linear nonrigid model accurately predicts large, nonrigid vertical displacement of plasma boundary produced in DIII-D experiment.

nonlinear current demand management near these limits have been designed and implemented on DIII-D. Such solutions are of even greater importance to devices such as ITER, which has a highly constrained performance envelope and will require reliable shape control even near coil current limits.

The algorithms developed at DIII-D adaptively compute a nominal coil current trajectory vector to minimize the proximity to limits while still maintaining good shape control. The approach takes advantage of the fact that in a device with more PF-coils than parameters to be controlled, there exists a subspace of coil current vectors that will not affect the plasma shape. Coil current vectors in this "shape nullspace" can be added to the equilibrium current vector to move it away from current limits.

We define I_{center} to be the vector of currents which are midway between the minimum and maximum current values for each PF coil. Given a measured current I_{meas}, we wish to find a minimizing nominal current vector I_{nom} such that it produces the same error signal as I_{meas}. The weight W is used to account for the fact that different coils have different allowable coil current ranges. This problem reduces to solving the optimization problem

$$\min_{q} \left\| W\left(P_{N^{\perp}}(I_{meas} - I_{center}) + X_N(q - q_{center})\right)\right\|^2 \tag{10}$$

where X_N is the matrix of orthonormal basis vectors for the shape nullspace N, $N^{\perp}$ refers to the current vector space which does affect the shape, $P_{N^{\perp}}$ is the projection of the current vector space onto $N^{\perp}$, q is the vector of coefficients of the shape nullspace basis vectors, and $q_{center} = X_N^I I_{center}$. The problem (10) has the solution $q = Q(I_{meas} - I_{center}) + q_{center}$ where $Q = -(WX_N)^{\dagger} WP_{N^{\perp}}$ where the dagger represents the pseudoinverse. Then $I_{nom} = P_{N^{\perp}} I_{meas} + X_N q$ is the desired nominal current. The resulting control approach is described schematically in Figure 5. The original control approach simply feeds back flux errors at DIII-D shape control points near the plasma boundary. The new algorithm regulates the coil currents as well through a separate path to calculate the nominal coil current trajectory.

Figure 6 illustrates this process in simulation for a single coil that tends to fall to a current level near zero, which represents a current limit for DIII-D voltage sources ("Experimental current"). The current evolution produced in simulation closely follows the calculated nominal value ("calculated nominal current trajectory"), which is near the current level midway between the maximum and minimum limits.

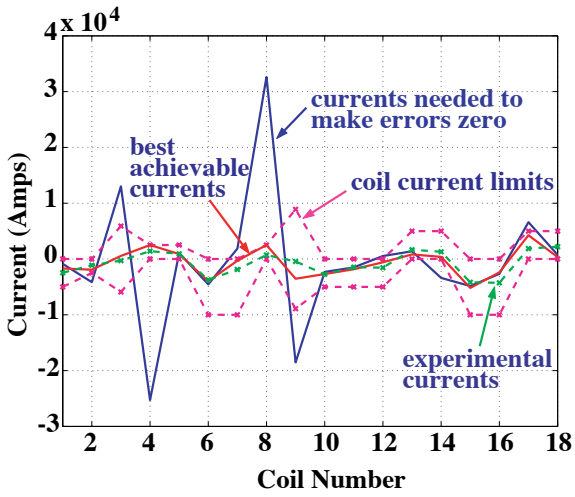

Fig. 4. Exactly matching an equilibrium shape request causes coil currents to exceed their operational limits.

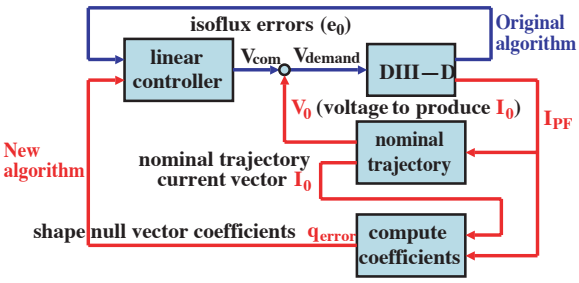

Fig. 5. Diagram of nonlinear current limit-mitigation scheme, illustrating feedback regulation of PF coil currents based on nonlinear nominal trajectory calculation.

5. Realtime Safety Factor Feedback for NTM Suppression

Development of the NTM suppression control system for DIII-D [1] provides an example of the integrated plasma control process applied to a nonaxisymmetric MHD control problem. NTM islands can be suppressed by replacing the bootstrap current deficit with ECCD current driven at the island q-surface. Alignment of the island and ECCD deposition locations must be achieved and maintained with an accuracy better than ~1-1.5 cm to produce satisfactory suppression. The degree of misalignment can be inferred from variations in fast magnetic measurements (reflecting island size) as the relative locations of island and ECCD are varied, or can be directly measured using a new facility for realtime q-profile reconstruction. A simplified version of the modified Rutherford equation (MRE) [14] was used to model the island response to ECCD in simulations to test controller operation.

major radial position, the toroidal field, or the plasma vertical position in order to produce alignment of the island and ECCD deposition location. The Search and Suppress algorithm scans one of these control quantities in discrete steps, with pauses to assess the effect on the island size (inferred from the RMS amplitude of high frequency magnetic measurements). Successful suppression results in a freeze of the control quantity and an activation of the Active Tracking algorithm, which seeks to keep the resonant surface at the location that produced mode suppression, even after the mode is gone.

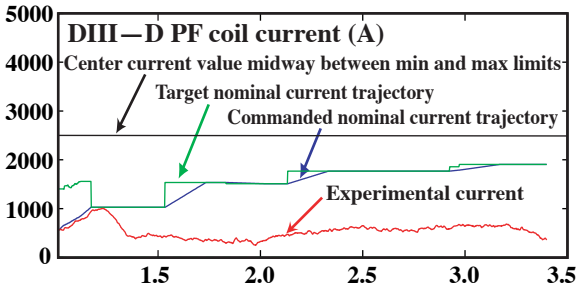

Fig. 6. Illustration of nominal current trajectory tracking to increase linear controller headroom and minimize likelihood of coil current limiting.

Prior to the 2004 run campaign, this tracking function made use of a neural network predictor to estimate the deviations from alignment after the mode was suppressed. Recently the realtime equilibrium reconstruction algorithm (RTEFIT) has been upgraded to provide realtime safety factor (q) calculation based on motional Stark effect (MSE) [15] and magnetic measurements. The Active Tracking algorithm can now use the realtime determination of the q-surface geometry to maintain alignment after the mode has been suppressed, or to prevent NTM onset. The optimal alignment can be determined either by empirical scans of the control parameter, through predictive calculation of the deposition location with the GA-TORAY [16] code, or through Search and Suppress action. Fig. 7 shows results of a DIII-D experiment in which the plasma major radius was set at a previously determined location producing good initial island-ECCD alignment, and the 3/2 mode was prevented from growing as the beam power was increased [Fig. 7(a)] to increase the normalized beta beyond the stability limit [Fig. 7(b)]. Figure 7(c) shows that the new q-surface feedback algorithm successfully held the major radius of the 3/2 surface ($R_{q=3/2}$) at the deposition location (Target ECCD), fixed in the lab frame. Maintaining this constant alignment required modifying the plasma major radius (R_{SURF}) by several cm.

6. Summary and Conclusions

Several new elements of the DIII-D integrated plasma control suite illustrate the wide range of applicability and maturity of the approach. A new nonrigid linear plasma response model based on linear perturbation of the Grad-Shafranov equation describes the plasma response more accurately than rigid models. New nonlinear algorithms for minimizing current limiting in DIII-D have also been developed, expanding the control headroom available to the PF coils. A new capability of reconstructing the geometry of internal safety factor surfaces in realtime has been used to improve NTM stabilization in DIII-D. DIII-D integrated plasma control tools are of specific value to next-generation device designs such as ITER, since their validation on DIII-D provides confidence in controller performance prior to experimental use.

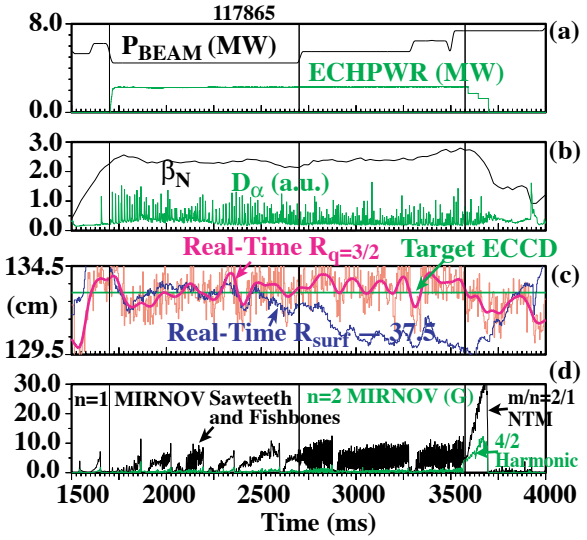

Fig. 7. Summary of DIII-D experiment in which initial optimal alignment of ECCD and island (q=1.5) surface is maintained using q-feedback active tracking. Mode onset is prevented (d), while power is increased (a), the normalized beta is raised (b), and alignment is maintained through radial displacement of the entire plasma by several cm (c).

Acknowledgment

Work supported by U.S. Department of Energy under Contract No. DE-FC02-04ER54698.

References

[1] LAHAYE, R.J., *et al.*, "Control of Neoclassical Tearing Modes in DIII-D," Phys. of Plasmas **9** (2002) 2051

[2] PENAFLOR, B.G., FERRON, J.R., JOHNSON, R.D., PIGLOWSKI, D.A., "Current Status of DIII-D Plasma Control System Computer Upgrades," Proc. 4th IAEA Technical Meeting on Control, Data Acquisition and Remote Participation for Fusion Research, San Diego, California, July 21-23, 2003; submitted to Fus. Eng. and Design.

[3] SYNAKOWSKI, E.J., "The National Spherical Torus Experiment (NSTX) Research Program and Progress Towards High Beta, Long Pulse Operating Scenarios," Proc. 19th IAEA Fusion Energy Conference, Lyon, France, October 2002, OV/2-2.

[4] KWON, M., BAK, J., LEE, G.-S., "Progress of the KSTAR Tokamak Engineering," Fus. Sci. and Tech. **42** (2002) 167.

[5] WAN, Y.X., WENG, P.D., LI, J.G., YU, Q.Q., GAO, D.M., HT-7U TEAM, "HT-7U Superconducting Tokamak," Proc. 19th IAEA Fusion Energy Conference, Lyon, France, October 2002, FT/P2-03.

[6] WALKER, M.L., HUMPHREYS, D.A., FERRON, J.R., "Control of Plasma Poloidal Shape and Position in the DIII-D Tokamak," Proc. 36th IEEE Conf. on Decision and Control, San Diego, CA (1997) 3703.

[7] WALKER, M.L., HUMPHREYS, D.A., JOHNSON, R.D., LEUER, J.A., "Nonlinear Methods for Current Limit Constraint Satisfaction," Proc. 16th Topical Meeting on Tech. of Fus. Energy (TOFE), Madison, WI, September 2004, P-II-9.

[8] FERRON, J.R., WALKER, M.L., LAO, L.L., STJOHN, H.E., HUMPHREYS, D.A., LEUER, J.A., "Realtime Equilibrium Reconstruction for Tokamak Discharge Control," Nucl. Fus. **38** (1998) 1055.

[9] AYMAR, R., CHUYANOV, V.A., HUGUET, M., SHIMOMURA, Y., ITER Joint Central Team, ITER Home Teams, "Overview of ITER-FEAT – The Future International Burning Plasma Experiment," Nucl. Fus. **41** (2001) 1301.

[10] KHAYRUTDINOV, R.R., LUKASH, V.E., "Studies of Plasma Equilibrium and Transport in a Tokamak Fusion Device with the Inverse-Variable Technique," J. Comput. Phys **109** (1993) 193.

[11] JENSEN, T.H., MCCLAIN, F.W., "Axisymmetric Control of Large Tokamak Devices," J. Plasma Phys. **32** (1984) 399.

[12] ALBANESE, R., COCCORESE, E., RUBINACCI, G., "Plasma Modeling for Vertical Instabilities," Nucl. Fusion **29** (1989) 1013.

[13] HUMPHREYS, D.A., HUTCHINSON, I.H., "Axisymmetric Magnetic Control Design in Tokamaks Using Perturbed Equilibrium Plasma Response Modeling," Fus. Tech. **23** (1993) 167.

[14] HEGNA, C.C., CALLEN, J.D., Phys. Pl. **4** (1997) 2940.

[15] RICE, B.W., NILSON, D.G., BURRELL, K.H., LAO, L.L., "Simultaneous Measurement of q and Er Profiles Using the Motional Stark Effect in High-Performance DIII-D Plasmas," Rev. Sci. Instr. 70 (1999) 815.

[16] KRITZ, A.H., et al, Proc. 3rd International Symposium on Heating in Toroidal Plasmas, Grenoble, Italy, 1982 (ECE, Brussels, 1982) vol. 2, p. 707.